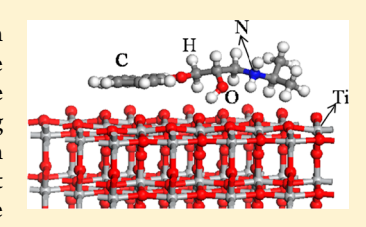
Insights into Propranolol Adsorption on TiO₂: Spectroscopic and **Molecular Modeling Study**

Cong Ye, † Shan Hu, † Wei Yan, † Jinming Duan, ‡ and Chuanyong Jing*, †

Supporting Information

ABSTRACT: Insights from molecular-level mechanisms of propranolol adsorption can further our understanding of the fate and transport of beta blockers in the environment. The motivation of our study is to explore the dynamic adsorption process of propranolol at the TiO₂/aqueous interface on the molecular scale. Multiple complementary techniques including macroscopic adsorption experiments, flow-cell ATR-FTIR measurement, XPS, and quantum chemical calculations were used to study the adsorption mechanisms. Our results show that propranolol adsorption on TiO₂ increased from 0.3 to 2.3 μ mol/g in the pH range 5 to 9. The ATR-FTIR and XPS analysis indicated that the hydroxyl and amino groups of propranolol



strongly interacted with the TiO₂ surface. The DFT calculations suggested the molecular structure of surface complexes with hydrogen bonding and the charge transfer from propranolol to TiO₂ surface upon adsorption.

■ INTRODUCTION

Propranolol is the first successful beta blocker developed to treat high blood pressure and cardiovascular diseases. The ubiquitous occurrence of propranolol in aquatic environment² and potential harm to organisms^{3–5} motivate extensive study in its adsorption behaviors, $^{2,6-8}$ which determine its transport and bioavailability. Propranolol exists as a positively charged species in natural environments with a pK_a of 9.53 (Figure S1, Supporting Information) and behaves like a cation at the aquatic-mineral interface. Previous study reports that hydrophobic, electrostatic, and chemical specific interactions play important roles in the uptake of propranolol by sediment/soil. However, different propranolol surface configurations are proposed. The uncharged surface complexes are suggested in the adsorption of three beta blockers including propranolol on iron-containing natural geosorbents.⁷ In contrast, positively charged surface species are assumed to dominate the adsorption of nine beta blockers on two sediments.² The difference in explaining macroscopic adsorption behaviors highlights the need to investigate the adsorption mechanism of propranolol on the molecular level.

The wide application of TiO₂ has made it inevitably enter the environment and consequently impact the fate and transport of organic pollutants. TiO₂ is one of the most investigated and understood metal oxides. ^{9,10} Compared with other metal oxides in sediments, TiO2 is chemically more stable and has a large number of active sorption sites on its surface due to its nanometer-scale particle size. Adsorption mechanism of organic molecules on ${
m TiO_2}$ has been investigated by spectroscopy studies and theoretical calculations on the molecular level. $^{11-13}$ Spectroscopic measurements are sensitive to surface reactions, and complementary quantum chemical calculations using periodical density functional theory (DFT) can assist in

interpreting the interactions between adsorbate and surface.¹³ However, no such integrated attempts have been reported to explore the mechanisms of propranolol adsorption on TiO₂.

The objective of this study was to explore the adsorption mechanism of propranolol on TiO2 on the molecule level. Multiple complementary techniques including batch adsorption experiments, in situ flow-cell attenuated total reflectance Fourier transform infrared (ATR-FTIR) measurements, X-ray photoelectron spectroscopy (XPS), surface complexation modeling, and periodic DFT calculations were used to gain insights into the adsorption process. The results should further our understanding of the retention mechanisms, fate, and transport of propranolol and similar pharmaceuticals in aquatic systems.

■ EXPERIMENTAL AND THEORETICAL METHODS

Materials. Propranolol hydrochloride (purity ≥99%, GR) was used as received from Acros Organics (New Jersey, USA). NaCl (Sinopharm Chemical Reagent Co., China) was used as background electrolyte. The TiO2 in anatase phase was prepared by hydrolysis of titanyl sulfate at 4 °C.14 The BET surface area was 196 m²/g, and the point of zero charge was 5.8. Milli-Q water was used in all experiments.

Batch Experiments. Adsorption isotherms at pH 5, 7, and 9 were established by transferring 20 mL of solution containing increasing amount of propranolol to polypropylene centrifuge tubes containing 0.1 g of TiO2 with a background electrolyte of 0.01 and 0.1 M NaCl. All tubes were then sealed and covered

Received: December 11, 2012 Revised: February 22, 2013 Published: February 27, 2013

[†]State Key Laboratory of Environmental Chemistry and Ecotoxicology, Research Center for Eco-Environmental Sciences, Chinese Academy of Sciences, Beijing 100085, China

[‡]School of Environmental and Municipal Engineering, Xi'an University of Architecture and Technology, Xi'an 710055, China

with aluminum foil. The samples were rotated end-over-end at 35 rpm for 24 h at 25 °C before soluble propranolol analysis.

Adsorption envelope experiments were performed to determine the adsorption edge, which is the percentage of propranolol adsorbed as a function of the final pH. Suspensions containing 6 mg/L propranolol and 5 g/L $\rm TiO_2$ were adjusted to desired pH values from 3 to 11 with NaOH and HCl. The background electrolyte was 0.01 M NaCl throughout the pH range. The samples were then processed in the same way with the isotherm experiments. Blank experiments without $\rm TiO_2$ were conducted in the same condition to minimize the influence of other factors.

The zeta potential was determined for blank ${\rm TiO_2}$ and propranolol adsorbed ${\rm TiO_2}$ as detailed in the Supporting Information. A charge distribution multisite complexation (CD-MUSIC) model was used to simulate the pH edge and zeta potential results as shown in the Supporting Information.

In Situ ATR-FTIR Spectroscopic Study. ATR-FTIR measurements were conducted using a Thermo-Nicolet Nexus 6700 FTIR spectrometer equipped with an ATRMax II horizontal flow cell (PIKE Tech., USA) and a liquidnitrogen-cooled mercury—cadmium—telluride (MCT) detector. The TiO₂ film was coated on the ZnSe crystal following the technique described by Voegelin and Hug with minor modifications. 15 Briefly, 300 µL of 3.5 g/L TiO₂ suspension was spread on the surface of the crystal and air-dried overnight. The crystal was gently rinsed with 0.01 M NaCl to flush out the uncoated particles and other impurities. The background solution of 0.01 M NaCl was flowing over the film at a rate of 0.3 mL/min for 3 h to reach equilibrium. The background solution was then replaced with 1 mM propranolol in 0.01 M NaCl at the same pH value. Spectra were recorded as a function of time until the adsorption reached equilibrium (approximately 3 h) using 256 scans at 4 cm⁻¹ resolution. No baseline correction or smoothing was applied to any spectrum.

X-ray Photoelectron Spectroscopy (XPS) Study. XPS analysis was conducted to examine the adsorbed propranolol on TiO₂ at pH 6.5 and 10. Suspensions containing 1 mM propranolol, 0.01 M NaCl, and 20 g/L TiO₂ were adjusted to pH 6.5 and 10 with HCl and NaOH. After mixing on a rotator for 6 h, the suspension was filtered, and the solids were freezedried under a vacuum chamber. XPS data was collected with an ESCALab220i-XL electron spectrometer from VG Scientific using 300 W Al K α radiation. The base pressure was about 3 × 10⁻⁹ Pa. The binding energies were referenced to the C 1s line at 284.8 eV from adventitious carbon. XPS data process and peak fitting were performed using the XPSPeak software package.

Molecular Model. The simulation of propranolol adsorption on TiO_2 surfaces was performed by the density functional theory program Castep¹⁶ in Materials Studio (Accelrys, San Diego, CA). Exchange and correlation interaction was described using the generalized gradient approximation (GGA) approach with the functional parametrized by Perdew–Burke–Ernzerhof (PBE).¹⁷ Ultrasoft pseudopotentials and plane-wave cutoff energy of 260 eV were adopted during geometry optimizations. To improve the estimation of energy and thermochemical property, a cutoff of 300 eV was subsequently used in the single-point energy calculation.¹⁸ The SCF tolerance was set to 1×10^{-6} eV/atom, and gamma point¹⁸ was used in all computations.

The bulk unit cell of anatase TiO_2 was first geometry optimized, and the obtained lattice parameters were a=b=

3.794 Å and c = 9.848 Å, in good agreement with experimental observations. After the (101) surface was cleaved, a three-layer slab was extracted, and a 3 \times 4 supercell was built. A vacuum of 20 Å was used to separate the periodic slab in the Z direction. The top layer of the surface was allowed to relax, and the rest of the two layers were kept frozen during the optimization process.

Propranolol molecule was geometry optimized in a periodic box of 20 Å side-length. The optimized molecule was then added to ${\rm TiO_2}$ to build an initial configuration that the amino and hydroxyl groups were oriented to the surface to calculate the adsorbed propranolol structure. The adsorption energy ($E_{\rm ads}$, in eV) of propranolol on ${\rm TiO_2}$ surface was calculated according to the following equation:

$$E_{\text{ads}} = E_{\text{prop@TiO2}} - (E_{\text{TiO2}} + E_{\text{prop}}) \tag{1}$$

where $E_{\text{prop@TiO2}}$, E_{TiO2} , and E_{prop} represents the energy of the surface complex, the TiO_2 surface, and the propranolol molecule, respectively.

The electron density difference $(\Delta \rho)$ was calculated to reveal the change of electron density during adsorption:²⁰

$$\Delta \rho = \rho_{\text{prop+TiO2}} - \rho_{\text{TiO2}} - \rho_{\text{prop}} \tag{2}$$

where $\rho_{\text{prop+TiO2}}$, ρ_{TiO2} and ρ_{prop} represents the electron density of the surface complex, the TiO_2 surface, and the propranolol molecule, respectively.

■ RESULTS AND DISCUSSION

Batch Adsorption Experiments. The adsorption of propranolol on TiO_2 was highly pH-dependent in the pH range of 4 to 11 (Figure 1). The increased adsorption as a

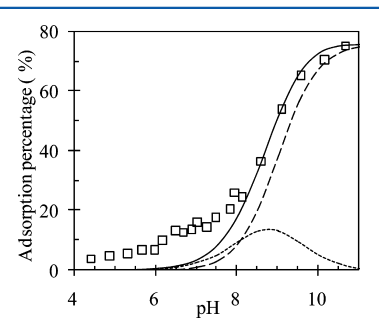


Figure 1. Experimental results (\square) and CD-MUSIC modeling (solid line) of 2.03×10^{-5} M (6 mg/L) propranolol adsorption on 5 g/L TiO₂ as a function of pH in 0.01 M NaCl solution. The dotted line (dashed line) represents the outer-sphere (inner-sphere) adsorption model.

function of pH can be attributed to the pH-dependent change of propranolol speciation (Figure S1, Supporting Information) and TiO_2 surface charge. At pH < pH_{pzc} (5.8), both the TiO_2 surface and propranolol were positively charged, and the electrostatic repulsion resulted in a low adsorption capacity. At pH_{pzc} < pH < pK_a (9.53), the TiO_2 surface was negatively charged, and propranolol was positively charged. The electrostatic attraction led to an enhanced adsorption affinity. At pH > pK_a, propranolol exists mainly in an uncharged species, resulting in a reduced adsorption. Therefore, electrostatic interactions play an important role in the adsorption of propranolol on TiO_2 .

However, electrostatic interactions alone cannot explain the observed adsorption in the pH range 4 to 5.8, where both

surface and propranolol were positively charged, and at pH > 9.53, where propranolol mainly exists as a neutral form. Interactions other than electrostatic force would be involved in propranolol adsorption on TiO_2 .

Adsorption isotherms of propranolol on TiO_2 at pH 5, 7, and 9 in the presence of 0.01 and 0.1 M NaCl followed the Freundlich model (Figure 2):

$$q = K_{\rm d}C^{1/n} \tag{3}$$

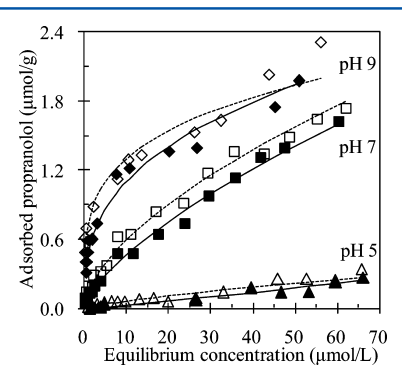


Figure 2. Adsorption isotherms of propranolol on 5 g/L TiO₂ at pH 5 (\triangle), pH 7 (\square), and pH 9 (\Diamond) in 0.01 M (open symbols) and 0.1 M NaCl (closed symbols) solution. Dashed (solid) lines are Freundlich models in the presence of 0.01 (0.1) M NaCl.

where $q (\mu \text{mol/g})$ is the amount of adsorption, $C (\mu \text{mol/L})$ is the aqueous propranolol concentration, K_d is the distribution coefficient, and 1/n is a correction factor, the deviation of which from 1 indicates the extent of nonlinearity. The best-fit Freundlich parameters are listed in Table S1, Supporting Information. As shown in Figure 2 and Table S1, Supporting Information, the maximum adsorption capacity was a function of pH, which was consistent with the pH edge results. The 1/nvalues were in the range 0.25 to 1.17, indicating that the adsorption of propranolol was nonlinear. The nonlinearity in adsorption isotherms may be partly attributed to heterogeneous adsorption sites and sorbate-sorbate interactions including electrostatic repulsion.²¹ In this study, the repulsive electrostatic interactions among cationic propranolol may exist due to its high surface loading (0.07 molecule/nm²). Moreover, the large molecular size of propranolol (about 1.4 nm) may lead to the steric exclusion or obstruction. In addition, ionic strength had a negligible effect on the adsorption of propranolol (Figure 2), suggesting the involved adsorption driving force was stronger than electrostatic interaction. Generally, electrostatic interaction is significantly influenced by ionic strength, whereas innersphere surface complexes should not vary as a function of ionic strength.22

ATR-FTIR Analysis. To study the interactions of propranolol with ${\rm TiO_2}$ on the molecule level, in situ flow-cell ATR-FTIR spectra were collected at pH 5, 7, and 9 as a function of time, and the results are shown in Figure 3. The time-dependent spectra are shown in Figure S3, and the peak positions and the assignments are listed in Table S2, Supporting Information.

The peak intensity increased as a function of time and pH (Figures 3 and S3, Supporting Information), while the shape of the spectra did not change. The spectrum of adsorbed propranolol at pH 9 exhibited a strong similarity with that of soluble propranolol (Figure 3). Meanwhile, peak shifts were

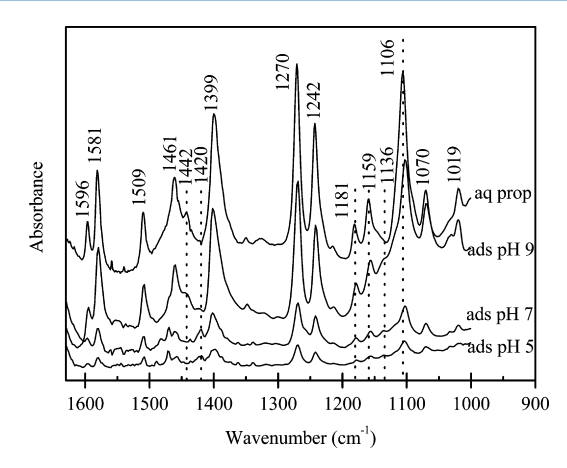


Figure 3. ATR-FTIR spectra of aqueous and adsorbed propranolol at pH 5, 7, and 9 in the 1000–1600 cm⁻¹ range.

observed for C-N and C-O bands. The C-N stretching band at 1181 cm⁻¹ in propranolol solution^{23,24} was shifted to 1178 cm⁻¹ upon adsorption. The magnitudes of the shift were considerably lower than that in the formation of inner-sphere surface complex.²⁵ This peak shift may be attributed to the hydrogen bonding between the $-NH_2^+$ group in propranolol and the negative TiO2 surface sites at pH 9. The C-O stretching vibrations at about 1159, 1106, and 1147 cm⁻¹ in propranolol²⁶ were shifted to 1156, 1102, and 1136 cm⁻¹, respectively, upon adsorption. Corresponding to the C-O band shift, the sharpness of the O-H bending vibration²⁷ at 1442 cm⁻¹ was decreased. The changes in C-O stretching and O-H bending vibrations were attributed to the hydrogen bonding of hydroxyl group in propranolol on TiO2 surfaces. 25,28 The changes in peak positions upon adsorption at pH 9 were also observed at pH 5 and 7 during the whole process of adsorption (Figure 3). The O-H bending vibration at 1442 cm⁻¹ in propranolol standard was shifted to 1420 cm⁻¹ at pH 5 and 7. Similar to pH 9, the bands at 1159, 1147, and 1106 cm⁻¹ due to C-O stretching were shifted to 1156, 1136, and 1102 cm⁻¹, respectively. The shift of O-H bending and C-O stretching vibrations indicated a strong hydrogen bonding between the -OH of propranolol and TiO₂ surface. In addition, the C-N stretching band shift was observed at pH 5 and 7, confirming the hydrogen bonding between the $-NH_2^+$ group and the surface.

The FTIR results indicated that the hydroxyl and amino group of propranolol interacted with TiO₂ surface at pH 5 to 9. The hydrogen bonding between the $-NH_2^+-$ group of propranolol and the TiO₂ surface would increase from pH 5 to 9 due to the decreasing positive charge of TiO2 surface (pH_{pzc} = 5.8). Meanwhile, a pronounced shift in O-H bending vibration suggested that interactions between hydroxyl group of propranolol and the surface may be the dominant adsorption mechanism at pH 5 to 7. Moreover, the peak shift due to hydrogen bonding between the hydroxyl group of propranolol and the TiO₂ surface was about 10–20 cm⁻¹, suggesting strong interactions comparable with inner-sphere surface complexes. In fact, hydrogen bond is partly covalent²⁹ and could exhibit covalent bond characters.^{30,31} Besides, the amino group and hydroxyl group of propranolol interacted with TiO2 surface simultaneously, which enhanced the affinity of propranolol to TiO2. The ATR-FTIR results indicated the interaction of -NH₂⁺- and -OH of propranolol with the TiO₂ surface, and

detailed information regarding the chemical and electronic states of N, O, and Ti at the interface merit the XPS study.

XPS Analysis. The binding energies of Ti $2p_{1/2}$ and Ti $2p_{3/2}$ for pristine TiO₂ were observed at 464.4 and 458.7 eV, respectively. No striking shift in the Ti peaks was detected upon adsorption at pH 6.5 and pH 10, respectively (Figure 4A). The spin—orbit splitting (SOS) of 5.7 eV between Ti $2p_{1/2}$ and $2p_{3/2}$ was in good agreement with previous study.³²

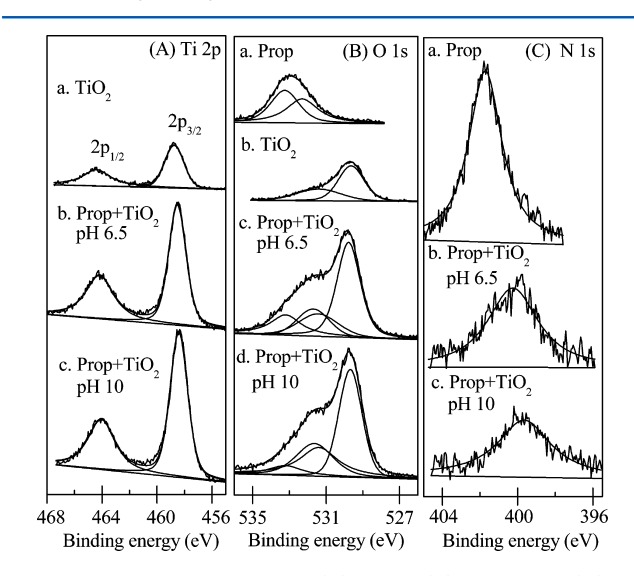


Figure 4. XPS spectra of Ti 2p (A), O 1s (B), and N 1s (C) for propranolol, TiO₂, and propranolol on TiO₂ at pH 6.5 and 10.

The peak shifts in the O 1s spectra implied that the hydroxyl group of propranolol interacted with the surface (Figure 4B). The peak at 533.2 and 532.3 eV (Figure 4B-a and Table1) was attributed to the O atom bonding to the naphthalene ring³³ and the O atom in the hydroxyl group³⁴ of propranolol, respectively. Two O 1s peaks were observed for TiO2 (Figure 4B-b) where the peak at 529.6 eV was attributed to lattice O atom (O²⁻), and the peak at 531.4 eV was assigned to the O atom in the surface hydroxyl group.³⁵ Upon adsorption at pH 6.5 and 10 (Figure 4B-c,d), the peak for the O associating naphthalene ring (533.2 eV) showed no change, whereas the O peak for the hydroxyl group in propranolol decreased from 532.3 eV to about 531.7 eV (pH 6.5) and 531.6 eV (pH 10). The decrease in binding energy suggested that the O atom in the hydroxyl group of propranolol accepted electrons upon adsorption on TiO2.

Analysis of the N 1s spectra supported the contribution of the $-\mathrm{NH_2}^+-$ group to the propranolol adsorption. The N 1s peak of propranolol was observed at 401.7 eV (Figure 4C-a), which was consistent with the reported value of $-\mathrm{NH_2}^+-$. Upon adsorption at pH 6.5 and 10, the binding energy of N 1s

decreased to 400.2 and 399.7 eV, respectively (Figure 4C-b,c). The decrease in the N 1s binding energy indicated that the nitrogen atom of propranolol accepted electrons and led to a less electron deficient environment upon adsorption. This binding energy change was attributed to the hydrogen bonding between the amino group of propranolol and ${\rm TiO_2}$ surface, in agreement with our ATR-FTIR results.

Surface Complexation Modeling. CD-MUSIC model was used to describe the adsorption behaviors including pH edge (Figure 1) and zeta potential curves (Figure 5).

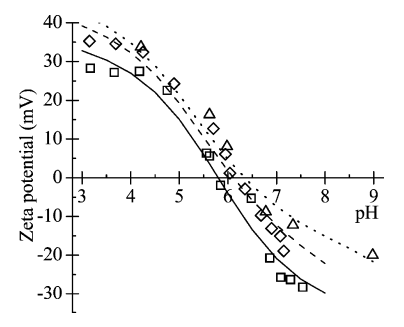


Figure 5. Experimental results and CD-MUSIC modeling of zeta potential for 0.2 g/L TiO_2 as a function of pH in 0 (\square , solid line), 0.12 mM (\Diamond , dashed line), and 1.2 mM (\triangle , dotted line) propranolol solution, respectively.

Consistent with our spectroscopic results, inner-sphere and outer-sphere complexes were included in the model calculation as listed in Table S3, Supporting Information, where the surface parameters and species were also specified.

Figure 5 shows the observed and model-simulated zeta potentials of ${\rm TiO_2}$ in the presence of 0.12 or 1.2 mM propranolol. The point of zero charge pH (pH_{pzc}) was shifted from 5.8 in pristine ${\rm TiO_2}$ to 6.1 in the presence of 0.12 mM propranolol. Upon an increase in propranolol concentration to 1.2 mM, the pH_{pzc} was shifted to 6.4, suggesting the formation of positively charged surface complexes. The calculated shift of pH_{pzc} was in good agreement with the experimental observation (Figure 5). The model could well simulate the adsorption pH edge curves (Figure 1). The double layer thickness of ${\rm TiO_2}$ (1/ κ) was calculated to be 3.04 nm, allowing propranolol (about 1.4 nm) to enter the inner-sphere of the ${\rm TiO_2}$ surface.

Quantum Chemical Calculations. Figure 6 presents the geometric optimized structure of propranolol on TiO₂ surface. The hydrogen end of amino and hydroxyl groups in propranolol molecule was oriented to the bridging oxygen atoms on the TiO₂ surface. The distance between the hydrogen atom in hydroxyl group and the surface oxygen atom was 1.6 Å, which is smaller than the sum of the van der Waals radius of hydrogen and oxygen atoms (2.6 Å), indicating the formation of hydrogen bond. The distance between the hydrogen atom in

Table 1. Ti 2p, O 1s, and N 1s Binding Energy (eV) Obtained from XPS Analysis

	Ti 2p		O 1s				N 1s
	2p _{1/2}	2p _{3/2}	C-O-C	С-ОН	ОН	O ²⁻	NH ₂ ⁺
$prop^a$			533.2	532.3			401.7
TiO_2	464.4	458.7			531.4	529.6	
Ads^b (pH 6.5)	464.2	458.5	533.2	531.7	531.4	529.8	400.2
Ads (pH 10)	464.1	458.4	533.2	531.6	531.4	529.7	399.7

^aPropranolol. ^bAdsorbed propranolol on TiO₂.

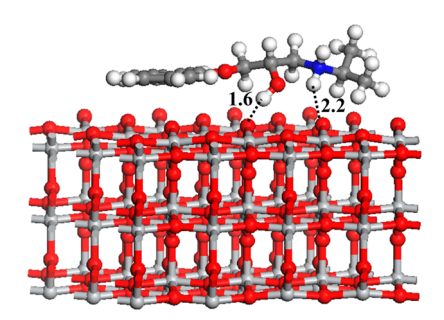


Figure 6. Geometric optimized structure of propranolol adsorption on $TiO_2(101)$ surfaces. Atoms are presented as dark gray (C), white (H), red (O), blue (N), and light gray (Ti). Distance in Å.

amino group and the surface oxygen atom was 2.2 Å, suggesting a weak hydrogen-bond interaction between the amino group of propranolol and the ${\rm TiO_2}$ surface. This adsorption model was in agreement with our ATR-FTIR results.

The calculated E_{ads} was -3.767 eV for the adsorption of propranolol on TiO2 surface. This large value of adsorption energy indicated strong interactions between adsorbent and adsorbate, confirming the inner-sphere complexes used in the CD-MUSIC model. Notably, the calculated E_{ads} was much larger than the sum of two hydrogen bonding energies (4-15 kcal/mol),³⁰ which may be explained from two aspects. First, the simplified model without considering solvation effect between adsorbent and adsorbate could lead to high E_{ads} . Water molecules may inhibit propranolol adsorption by trapping propranolol or capping the adsorption sites.²⁰ Second, the slab established in the model may not be large enough to eliminate potential interactions between the propranolol molecules, although the size of the slab (16.734 \times 15.191 \times 29.775 Å) was comparable to reported values. 18,20,37 Thus, molecular modeling considering the effect of solvation and slab size merits further research. Nevertheless, the results indicated that the hydrogen bonding of propranolol on the TiO₂ surface is energetically favorable and a stable inner-sphere surface complex could be formed.

The interaction between propranolol and TiO_2 induced the change in electron density of the surface and the adsorbate. In the electron density difference map (Figure 7), the yellow and

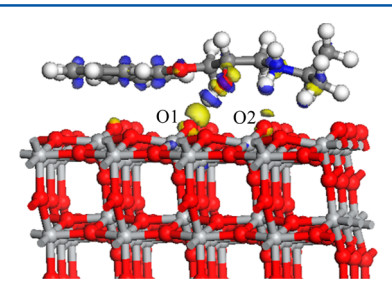


Figure 7. Electron density difference for propranolol on ${\rm TiO_2(101)}$ surface with the isovalues of $\Delta \rho = +0.02$ e (in blue) and -0.02 e (in yellow). Yellow represents charge accumulation, and blue represents charge depletion.

blue represents the charge accumulation and depletion, respectively. The charge accumulation occurred between the hydroxyl group of propranolol and the bridging-O (O1) atom of TiO₂. An increased electron density was also observed between the amino group and bridging-O (O2) atom. The charge depletion occurred near the H atoms in hydroxyl and

amino group bound to the surface. Moreover, the O atom in hydroxyl group and the N atom in amino group were in a state of electron density accumulation, which was in accordance with the decreased binding energy of the O 1s and N 1s in XPS results (Figure 4 and Table 1). Therefore, charge transfer possibly occurred from surface oxygen atoms to the hydroxyl and amino groups in propranolol. Interestingly, charge transfer between the naphthyl group and TiO2 surface was expected (Figure 7) where the naphthyl group acted as an electron donor and TiO2 surface as an electron acceptor. The UV-vis absorption spectra (Figure S4, Supporting Information) showed the change in peak intensity of propranolol upon adsorption, indicating that the TiO2 has interacted with propranolol and induced the electron transition of the naphthalene ring. However, the ATR-FTIR spectra did not exhibit relative changes, and we considered that the interaction between the naphthyl group and TiO2 surface plays a minor role in the adsorption of propranolol.

The density of states (\overline{DOS}) for propranolol adsorption on the $TiO_2(101)$ surface was calculated to characterize the interactions. Figure 8 shows the partial density of states

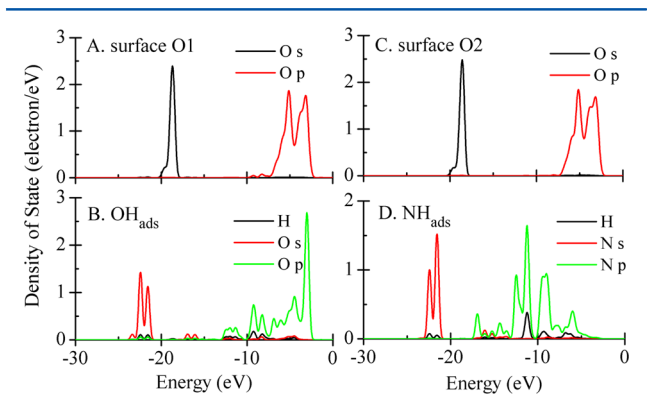


Figure 8. Partial density of states of propranolol on $TiO_2(101)$ surfaces: (A) surface O1, (B) hydroxyl group of propranolol, (C) surface O2, (D) amino group of propranolol. Surface O1 and O2 atoms are marked in Figure 7.

(PDOS) of adsorbed propranolol and $TiO_2(101)$ surface. The atomic orbitals of the hydroxyl group (Figure 8B) of adsorbed propranolol overlapped with the orbitals of the bridging-O (O1) atom (Figure 8A). This overlap demonstrated the formation of the bond between the hydroxyl group in adsorbed propranolol and TiO_2 surface. Similarly, overlaps between the atomic orbitals of the amino group (Figure 8D) of adsorbed propranolol and that of the bridging-O (O2) atom of the TiO_2 surface (Figure 8C) were observed with a less extent than that of the hydroxyl group and surface O atom orbitals. The analysis of PDOS was consistent with the result of electron density difference and demonstrated the specific interactions between propranolol and TiO_2 .

CONCLUSIONS

The ultimate fate of propranolol in the environment can be strongly influenced by its adsorption. In this study, the adsorption capacity of propranolol on ${\rm TiO_2}$ increases from 0.3 to 2.3 μ mol/g in the pH range 5 to 9. The DFT calculations agree well with our ATR-FTIR and XPS analysis and suggest the hydroxyl and amino groups of adsorbed propranolol strongly interact with the ${\rm TiO_2}$ surface. This strong affinity can slow the migration of propranolol and reduce the potential for

exposure. The interaction mechanisms at water—solid interfaces for propranolol may be safely extrapolated to other pharmaceuticals with the same functional groups. Although the solvation effect in DFT simulation and the supplement of calculated vibration to ATR-FTIR experiment need further investigation, the aquatic—mineral interface model established in this study can improve our understanding of the fate and risk assessment of propranolol and analogous compounds.

ASSOCIATED CONTENT

S Supporting Information

Kinetics experiment, porpanolol analysis, surface complexation modeling, electrophoretic mobility measurements, and UV—vis absorption spectroscopy study; tables showing Freundlich isotherm parameters, ATR-FTIR peak assignment of propranolol, and CD-MUSIC model parameters; figures showing structure and property of propranolol, adsorption kinetics, ATR-FTIR spectra of propranolol on TiO₂ as a function of time, UV—vis absorption spectra of propranolol on TiO₂, and partial density of states of propranolol on TiO₂. This material is available free of charge via the Internet at http://pubs.acs.org.

AUTHOR INFORMATION

Corresponding Author

*(C.J.) Tel: +86 10 6284 9523. Fax: +86 10 6284 9523. E-mail: cyjing@rcees.ac.cn.

Notes

The authors declare no competing financial interest.

ACKNOWLEDGMENTS

The molecular model results described in this article were obtained on the Deepcomp7000 of Supercomputing Center, Computer Network Information Center of Chinese Academy of Sciences. Support for this research was provided by National Natural Science Foundation of China (41023005, 20890112, and 20921063) and National Basic Research Program of China (2010CB933502).

REFERENCES

- (1) Stapleton, M. P. Sir James Black and Propranolol: The Role of the Basic Sciences in the History of Cardiovascular Pharmacology. *Texas Heart Inst. J.* **1997**, *24*, 336–342.
- (2) Ramil, M.; El Aref, T.; Fink, G.; Scheurer, M.; Ternes, T. A. Fate of Beta Blockers in Aquatic-Sediment Systems: Sorption and Biotransformation. *Environ. Sci. Technol.* **2010**, *44*, 962–970.
- (3) Franzellitti, S.; Buratti, S.; Valbonesi, P.; Capuzzo, A.; Fabbri, E. The β -Blocker Propranolol Affects CAMP-Dependent Signaling and Induces the Stress Response in Mediterranean Mussels *Mytilus Galloprovincialis*. Aquat. Toxicol. **2011**, 101, 299–308.
- (4) Giltrow, E.; Eccles, P. D.; Winter, M. J.; McCormack, P. J.; Rand-Weaver, M.; Hutchinson, T. H.; Sumpter, J. P. Chronic Effects Assessment and Plasma Concentrations of the β -Blocker Propranolol in Fathead Minnows (*Pimephales Promelas*). Aquat. Toxicol. **2009**, 95, 195–202.
- (5) Huggett, D. B.; Brooks, B. W.; Peterson, B.; Foran, C. M.; Schlenk, D. Toxicity of Select Beta Adrenergic Receptor-Blocking Pharmaceuticals (B-Blockers) on Aquatic Organisms. *Arch. Environ. Contam. Toxicol.* **2002**, 43, 229–235.
- (6) Yamamoto, H.; Nakamura, Y.; Moriguchi, S.; Nakamura, Y.; Honda, Y.; Tamura, I.; Hirata, Y.; Hayashi, A.; Sekizawa, J. Persistence and Partitioning of Eight Selected Pharmaceuticals in the Aquatic Environment: Laboratory Photolysis, Biodegradation, and Sorption Experiments. *Water Res.* **2009**, *43*, 351–362.

- (7) Kibbey, T. C. G.; Paruchuri, R.; Sabatini, D. A.; Chen, L. Adsorption of Beta Blockers to Environmental Surfaces. *Environ. Sci. Technol.* **2007**, *41*, 5349–5356.
- (8) Lin, A. Y. C.; Lin, C. A.; Tung, H. H.; Chary, N. S. Potential for Biodegradation and Sorption of Acetaminophen, Caffeine, Propranolol and Acebutolol in Lab-Scale Aqueous Environments. *J. Hazard. Mater.* **2010**, *183*, 242–250.
- (9) Mudunkotuwa, I. A.; Grassian, V. H. Citric Acid Adsorption on ${\rm TiO_2}$ Nanoparticles in Aqueous Suspensions at Acidic and Circumneutral PH: Surface Coverage, Surface Speciation, and Its Impact on Nanoparticle-Nanoparticle Interactions. *J. Am. Chem. Soc.* **2010**, *132*, 14986–14994.
- (10) Zhao, Z.; Li, Z.; Zou, Z. Structure and Properties of Water on the Anatase TiO₂ (101) Surface: From Single-Molecule Adsorption to Interface Formation. *J. Phys. Chem. C* **2012**, *116*, 11054–11061.
- (11) Li, C.; Monti, S.; Carravetta, V. Journey toward the Surface: How Glycine Adsorbs on Titania in Water Solution. *J. Phys. Chem. C* **2012**, *116*, 18318–18326.
- (12) Weston, M.; Reade, T. J.; Handrup, K.; Champness, N. R.; O'Shea, J. N. Adsorption of Dipyrrin-Based Dye Complexes on a Rutile TiO₂ (110) Surface. *J. Phys. Chem. C* **2012**, *116*, 18184–18192.
- (13) Almeida, A. R.; Calatayud, M.; Tielens, F.; Moulijn, J. A.; Mul, G. Combined ATR-FTIR and DFT Study of Cyclohexanone Adsorption on Hydrated ${\rm TiO_2}$ Anatase Surfaces. *J. Phys. Chem. C* **2011**, *115*, 14164–14172.
- (14) Luo, T.; Cui, J.; Hu, S.; Huang, Y.; Jing, C. Arsenic Removal and Recovery from Copper Smelting Wastewater Using TiO₂. *Environ. Sci. Technol.* **2010**, *44*, 9094–9098.
- (15) Voegelin, A.; Hug, S. J. Catalyzed Oxidation of Arsenic(III) by Hydrogen Peroxide on the Surface of Ferrihydrite: An in Situ ATR-FTIR Study. *Environ. Sci. Technol.* **2003**, *37*, 972–978.
- (16) Clark, S. J.; Segall, M. D.; Pickard, C. J.; Hasnip, P. J.; Probert, M. J.; Refson, K.; Payne, M. C. First Principles Methods Using CASTEP. Z. Kristallogr. 2005, 220, 567–570.
- (17) Perdew, J. P.; Burke, K.; Ernzerhof, M. Generalized Gradient Approximation Made Simple. *Phys. Rev. Lett.* **1996**, *77*, 3865–3868.
- (18) Ojamae, L.; Aulin, C.; Pedersen, H.; Kall, P. O. IR and Quantum-Chemical Studies of Carboxylic Acid and Glycine Adsorption on Rutile TiO₂ Nanoparticles. *J. Colloid Interface Sci.* **2006**, 296, 71–78.
- (19) Burdett, J. K.; Hughbanks, T.; Miller, G. J.; Richardson, J. W.; Smith, J. V. Structural—Electronic Relationships in Inorganic Solids: Owder Neutron Diffraction Studies of the Rutile and Anatase Polymorphs of Titanium-Dioxide at 15 and 295 K. *J. Am. Chem. Soc.* 1987, 109, 3639–3646.
- (20) Guo, Y.; Lu, X.; Zhang, H.; Weng, J.; Watari, F.; Leng, Y. DFT Study of the Adsorption of Aspartic Acid on Pure, N-Doped, and Ca-Doped Rutile (110) Surfaces. *J. Phys. Chem. C* **2011**, *115*, 18572–18581
- (21) Higgins, C. P.; Luthy, R. G. Sorption of Perfluorinated Surfactants on Sediments. *Environ. Sci. Technol.* **2006**, *40*, 7251–7256.
- (22) O'day, P. A. Molecular Environmental Geochemistry. *Rev. Geophys.* **1999**, 37, 249–274.
- (23) Castro, R. A. E.; Canotilho, J.; Nunes, S. C. C.; Eusebio, M. E. S.; Redinha, J. S. A Study of the Structure of the Pindolol Based on Infrared Spectroscopy and Natural Bond Orbital Theory. *Spectrochim. Acta, Part A* **2009**, *72*, 819–826.
- (24) Canotilho, J.; Castro, R. A. E. The Structure of Betaxolol Studied by Infrared Spectroscopy and Natural Bond Orbital Theory. *Spectrochim. Acta, Part A* **2010**, *76*, 395–400.
- (25) Johnson, S. B.; Yoon, T. H.; Kocar, B. D.; Brown, G. E. Adsorption of Organic Matter at Mineral/Water Interfaces. 2. Outer-Sphere Adsorption of Maleate and Implications for Dissolution Processes. *Langmuir* **2004**, *20*, 4996–5006.
- (26) Farooqi, Z. H.; AboulEnein, H. Y. IR and UV/Visible Spectra of Propranolol and Some Fluorinated Derivatives: Comparison of Experimental and Calculated Values. *Biospectroscopy* **1996**, 2, 131–141.

- (27) Sidiras, D.; Batzias, F.; Schroeder, E.; Ranjan, R.; Tsapatsis, M. Dye Adsorption on Autohydrolyzed Pine Sawdust in Batch and Fixed-Bed Systems. *Chem. Eng. J.* **2011**, *171*, 883–896.
- (28) Morrison, W. H. Aqueous Adsorption of Anions onto Oxides at PH Levels above the Point of Zero Charge. *J. Colloid Interface Sci.* **1984**, *100*, 121–127.
- (29) Isaacs, E. D.; Shukla, A.; Platzman, P. M.; Hamann, D. R.; Barbiellini, B.; Tulk, C. A. Covalency of the Hydrogen Bond in Ice: A Direct X-Ray Measurement. *Phys. Rev. Lett.* **1999**, *83*, 600–603.
- (30) Parthasarathi, R.; Subramanian, V.; Sathyamurthy, N. Hydrogen Bonding Without Borders: An Atoms-in-Molecules Perspective. *J. Phys. Chem. A* **2006**, *110*, 3349–3351.
- (31) Emsley, J. Very Strong Hydrogen-Bonding. Chem. Soc. Rev. 1980, 9, 91–124.
- (32) Fierro, J. L. G.; Arrua, L. A.; Nieto, J. M. L.; Kremenic, G. Surface Properties of Co-Precipitated V-Ti-O Catalysts and Their Relation to the Selective Oxidation of Isobutene. *Appl. Catal.* **1988**, *37*, 323–338.
- (33) delaPuente, G.; Pis, J. J.; Menendez, J. A.; Grange, P. Thermal Stability of Oxygenated Functions in Activated Carbons. *J. Anal. Appl. Pyrolysis* **1997**, *43*, 125–138.
- (34) Gleason, N.; Guevremont, J.; Zaera, F. Thermal Chemistry of 2-Propanol and 2-Propyl Iodide on Clean and Oxygen-Pretreated Ni(100) Single-Crystal Surfaces. *J. Phys. Chem. B* **2003**, *107*, 11133—11141.
- (35) Simmons, G. W.; Beard, B. C. Characterization of Acid–Base Properties of the Hydrated Oxides on Iron and Titanium Metal-Surfaces. *J. Phys. Chem.* **1987**, *91*, 1143–1148.
- (36) Li, P.; Lin, J.; Tan, K. L.; Lee, J. Y. Electrochemical Impedance and X-Ray Photoelectron Spectroscopic Studies of the Inhibition of Mild Steel Corrosion in Acids by Cyclohexylamine. *Electrochim. Acta* 1997, 42, 605–615.
- (37) Zhao, Z.; Li, Z.; Zou, Z. Understanding the Interaction of Water with Anatase TiO₂ (101) Surface from Density Functional Theory Calculations. *Phys. Lett. A* **2011**, 375, 2939–2945.